Radio Science

TECHNICAL REPORTS: METHODS
10.1029/2018RS006707

Key Point:
- During ExoMars Landing, GMRT observed UHF transmissions and Doppler shift used to identify key events as only real-time aliveness indicator

Correspondence to:
S. W. Asmar,
sami.w.asmar@jpl.nasa.gov

Citation:
Esterhuizen, S., Asmar, S. W., De, K., Gupta, Y., Katore, S. N., & Ajithkumar, B. (2019). ExoMars Schiaparelli Direct-to-Earth observation using GMRT. *Radio Science*, *54*, 314–325. https://doi.org/10.1029/2018RS006707

Received 8 AUG 2018
Accepted 9 JAN 2019
Accepted article online 15 JAN 2019
Published online 1 MAR 2019

ExoMars Schiaparelli Direct-to-Earth Observation using GMRT

S. Esterhuizen[1], S. W. Asmar[1], K. De[2], Y. Gupta[3], S. N. Katore[3], and B. Ajithkumar[3]

[1]Jet Propulsion Laboratory, California Institute of Technology, Pasadena, CA, USA, [2]Cahill Center for Astrophysics, California Institute of Technology, Pasadena, CA, USA, [3]National Centre for Radio Astrophysics, Pune, India

Abstract During the ExoMars Schiaparelli separation event on 16 October 2016 and Entry, Descent, and Landing (EDL) events 3 days later, the Giant Metrewave Radio Telescope (GMRT) near Pune, India, was used to directly observe UHF transmissions from the Schiaparelli lander as they arrive at Earth. The Doppler shift of the carrier frequency was measured and used as a diagnostic to identify key events during EDL. This signal detection at GMRT was the only real-time aliveness indicator to European Space Agency mission operations during the critical EDL stage of the mission.

Plain Language Summary When planetary missions, such as landers on the surface of Mars, undergo critical and risky events, communications to ground controllers is very important as close to real time as possible. The Schiaparelli spacecraft attempted landing in 2016 was supported in an innovative way. A large radio telescope on Earth was able to eavesdrop on information being sent from the lander to other spacecraft in orbit around Mars. This provided real-time (after accounting for one-way light time) basic information to mission controllers.

1. Introduction

The European Space Agency (ESA) ExoMars Trace Gas Orbiter (TGO) carried an Entry, Descent, and Landing (EDL) Demonstrator Module (EDM) called Schiaparelli. Measuring the performance of Schiaparelli during EDL will provide ESA valuable data for future missions to the surface of Mars. Unlike other recent missions to Mars' surface, Schiaparelli does not have Direct-to-Earth capability, and it relies on the Mars Orbiters to relay its UHF communications back to Earth.

JPL has supported EDL for various probes and landers via a Direct-To-Earth observation, this includes among others, the Huygens Titan Probe (Folkner et al., 2006; Witasse et al., 2006), Phoenix Mars Lander (Kornfeld et al., 2011), and Curiosity (Oudrhiri et al., 2013; Schratz et al., 2014; Soriano et al., 2013).

Due to orbiter geometry constraints, this critical EDL data would only be relayed back to Earth via the orbiters with a few hours of latency. The lowest latency observation possible was to directly observe this signal on Earth and relay detection status to ESA mission operations (ESOC; Asmar et al., 2017). Giant Metrewave Radio Telescope (GMRT) near Pune, India, was selected because it was uniquely located during the landing phase of Schiaparelli, where Mars was at favorable elevation angles as viewed from the facility.

The GMRT (Gupta et al., 2000) is a multielement aperture synthesis telescope, consisting of an array of 30 dishes, each with a diameter of 45 m, spread over a maximum baseline of ≈25 km (Swarup, 1997). The array mode can be configured to produce either an incoherent array beam, where the power signals from the antennas are directly added, or a phased array beam, where sampled voltages from the antennas are added after phase delay corrections. Both of these beam modes can be used to obtain high time resolution observations of the total received power (or four Stokes parameters), while the phased array mode also supports an option for recording the phase-corrected and added voltages in real time.

The high sensitivity of the GMRT at low frequencies allows one to use the interferometer for detection of weak radio signals, including those from appropriately configured transmitters on space-based interplanetary missions.

In this paper, we describe the results from an experiment conducted with the GMRT to track the Schiaparelli lander's UHF signal in real time. The experiment was accomplished using the phased array configuration of

the telescope in the raw voltage mode, followed by digital processing to produce very narrow spectral bins (around 1 Hz) to detect the very weak radio signals received on Earth.

2. Link Budget

Schiaparelli transmits at a nominal frequency of 401.585625 MHz at 4.8 W. During separation and the first part of EDL, the low gain antenna (LGA) on the entry vehicle backshell is used, the gain of this backshell antenna is 1–2 dBiC. After backshell jettison, the Schiaparelli lander's Surface Platform LGA is used, with peak gain of 6.2 dBiC.

The link budget is shown in Appendix A and summarized in Table A1. It is computed for the backshell LGA, optimistically assuming 2 dBiC gain toward Earth. In reality, during EDL, the total gain toward Earth will fluctuate between 2 and −6 dBiC using the backshell LGA as observed at GMRT. This change in gain is due to the pointing of the backshell LGA changing rapidly during the violent ride to the surface of Mars. Throughout nominal operations, only the "inner arm" of the GMRT array was used (12 antennas), the link budget reflects this number. The Carrier-to-noise-density ratio (C/No) is expected to be 7.7 dB-Hz at maximum LGA gain, but could be as low as −0.3 dB-Hz depending on GMRT viewing angle.

The UHF transmitter modulates the carrier with 60° modulation index. The carrier is reduced by 6 dB, leaving a residual carrier. It is this residual carrier that can be detected at Earth.

3. Signal Processing

An overview of the Digital Signal Processing chain can be seen in Figure A1. After digitization of N-antenna elements, the GMRT digital backend arrays these N signals in the frequency domain. A single beam is formed, passed through the real-time inverse FFT block. Once in the time domain, velocity and acceleration predicts are applied to effectively stop the signal. At this point, the signal goes through multiple stages of filtering and decimation to ultimately produce a 8 kHz bandwidth signal, centered close to the predicted Doppler frequency.

3.1. GMRT Software Backend

The high time resolution beam mode observations are facilitated by real-time signal processing with the GMRT Software Backend (Roy et al., 2010). The beam mode data are recorded as a time series with multiple spectral channels (typically with 256 or 512 channels) over a total bandwidth of up to 32 MHz. Additionally, the backend also supports a voltage-beam former mode, where the phase-corrected voltages from each antenna are added (in frequency domain) and directly sent to a recording server without squaring and integration. This facilitates the highest time resolution observations (up to 15 ns resolution for 32 MHz bandwidth) with the telescope. Each of the two polarization (left and right circularly polarized) signals are sent to two individual recording nodes, where a MPI-synchronized routine writes the voltage-beam data into a ring buffer in shared memory.

The format of the data is similar to the total intensity beam mode and contains the real and imaginary parts of the voltage time series for each frequency channel. The voltage data being written to the ring buffer in real time can be attached to a local process on the host machine to either record the raw voltage stream on to a disk, or perform additional signal processing for specific applications (e.g., coherent dedispersion; De & Gupta, 2016). In order to meet the requirements of the current project, we used the front end processing of the previously available real-time coherent dedispersion system, where the voltages in the spectral domain are transformed back to time domain using a parallelized real-time inverse FFT routine running on the server. The routine produces a real-time voltage time series (written as 4 byte binary floating point numbers), which is directed to the input of the EDL processing code via a shell pipe.

3.2. EDL Signal Processing

The Digital Signal Processing to support EDL has a few stages (Figure A2). For both polarizations the following is computed on the GMRT Node:

1. Convert Phased Array Voltage spectrum to time domain voltage.
2. Mix and decimate data to lower rate on GMRT nodes.
3. Transfer ≈ 0.5 Megabytes per second per polarization complex voltage time series data to EDL laptop.

The following steps are processed on the EDL laptop:

1. Apply velocity and acceleration corrections to account for geometry and predicted spacecraft maneuvers. These corrections are applied once per second.
2. Further reduce bandwidth to 8 kHz.
3. Display real-time spectrogram of 8,192 bins: ≈ 1 Hz FFT bin size.
4. Display real-time FFT with long averaging.

Once the resolution bandwidth is around 1 Hz, the noise in each frequency bin should be 7.7 dB lower than the predicted peak signal from Schiaparelli (see link budget in Appendix A). Due to signal fading, very low signal strength, unmodeled clock, and dynamics, it is not possible to perform closed loop tracking on the signal. It was decided to use a wide-bandwidth open loop approach: create spectrograms centered around the predicted frequency ±4 kHz. The predicted clock rate error and geometry error were not expected to exceed this spectral window. As backup, higher-bandwidth (256 kHz) data were also collected in case there was an unexpected frequency offset.

The final part of the signal detection is left to the EDL operator. With signals ranging from −0.3 to +7.7 dB-Hz, a sporadically detectable signal can be observed in real time on the spectrogram, as well as the long-averaging FFT.

4. Testing

The first test of the signal processing chain used tones injected at GMRT. This allowed the team to quickly test the signal flow and confirm correct mixing frequencies, etc.

After confirmation of correct tone processing, an end-to-end systems test was performed by detecting UHF transmissions from the Curiosity rover on the surface of Mars.

4.1. Listening to Curiosity/MSL on Mars

During August and October 2016, multiple tests were performed with the Curiosity rover (Mars Science Lab, MSL). These tests were designed to be nonintrusive and take advantage of already scheduled overflights with various orbiters. Good geometry for Mars UHF observation at GMRT is met when the following conditions are true:

1. UHF return link scheduled from MSL to Mars orbiter.
2. GMRT is visible from MSL.

This geometry is depicted in Figure A3. Only observations for MSL/ODY (Odyssey) are shown here. The newer orbiters use adaptive data rate for communications (Bell et al., 2014) and has no residual carrier to detect, except briefly when the adaptive data rate is negotiated.

The detected C/No for multiple observation campaigns are shown in Table A2. Because MSL's Rover UHF antenna has gain of 3 dBiC and transmit power is 10 W (Makovsky et al., 2009), we expect a C/No that is 4 dB higher than Schiaparelli, this translates to 12 dB-Hz using 12 GMRT antennas. The variation in C/No is partially explained by the elevation angle of Earth as viewed by Curiosity. The 23 and 25 August observations had Earth high up in the sky, while the 31 August observation had less favorable viewing conditions, with lower UHF antenna gain pointed toward the Earth.

The carrier for MSL was strong enough where a phased lock loop could be locked to the signal. This allowed us to check phase coherence of the array for the first time. Figure A4 shows tracking results for 7.5 min while MSL was communicating with ODY on 25 August 2016. An average C/No of 16.5 dB-Hz was measured. Note the smooth carrier phase after removing a fourth order polynomial from the observed carrier phase, a fourth order polynomial is selected to remove any unmodeled geometry and clock dynamics up to change in acceleration.

5. ExoMars Schiaparelli Observations

There were three opportunities where Schiaparelli turned on its UHF transmitter:

1. 21 September 2016: Schiaparelli still attached to TGO, transmitter on for 2 min separated by roughly 4 hr 30 min.

2. 16 October 2016: Schiaparelli separates from TGO, transmitter on for 30 min.
3. 19 October 2016: Schiaparelli lands on Mars, transmitter on for 1 hr 36 min.

GMRT did not detect any signals on 21 September 2016, but this was expected due to TGO blocking the UHF antenna on Schiaparelli. The authors successfully detected carrier from Schiaparelli during the 16 and 19 October 2016 events.

5.1. Time Stamps

All times in the following sections are either reported in UTC Earth Receive Time (ERT), which corresponds to when the signal arrived at Earth, or in UTC Spacecraft Event Time (SCET). These times are related to each other by the one-way light time. For separation on 16 October UTC(ERT) = UTC(SCET) + 576 s. For EDL on 19 October UTC(ERT) = UTC(SCET) + 587 s.

5.2. Separation—16 October 2016

On 16 October 2016, 3 days before Mars entry, when the Schiaparelli separated from TGO, the one-way light time was 576 s. The UHF transmitter on Schiaparelli was turned on for 30 min as per Table A3. The elevation angle and predicted Doppler can be seen in Figure A5. The spectrogram in Figure A6 shows signal detection at GMRT at 14:52:34 UTC ERT with Doppler shift of −18.43 kHz from the resting transmit frequency, or about −1.3 kHz from predicted. No predict model was applied, all frequency offsets reported relative to 401.585625 MHz, the rest frequency of the transmitter. The change in Doppler of 1.3 kHz over this observation is dominated by the onboard oscillator heating up.

After performing phase calibration on a nearby phase calibrator, the GMRT was pointed toward TGO/EDM using 18 antennas in the array. About 3.5 min into the detection, GMRT scanned the beam around TGO in an attempt to maximize C/No. The signal was observed until 15:06:31 UTC ERT, 9 s before the expected UHF transmitter off time.

This first detection of Schiaparelli allowed us to observe the transmit frequency offset from expected (due to Schiaparelli oscillator frequency drift). Comparing the predicted and measured Doppler shift, one can note the oscillator seems to undergo frequency fluxuations of 1,355 Hz (including geometry change which contributes about 100 Hz). This is expected behavior for an oscillator that has just been turned on. The peak C/No during this observation was 2.2 dB-Hz.

5.3. EDL—19 October 2016

After 3 days of coasting to Mars, Schiaparelli turned on its UHF transmitter an hour and 15 min before predicted atmospheric entry. Key events are outlined in Table A4. During this observation one-way light time was about 587 s, with good visibility from GMRT (see Figure A7). The predicted Doppler shift of the UHF signal as observed at GMRT will range from −21 to −14 kHz.

The carrier was successfully detected at approximately 13:40:31 UTC ERT (see Table A5), about 4 min after the transmitter was predicted to turn on. At this stage the C/No was barely 0.5 dB-Hz, possibly because of rapid changes in Doppler frequency due to the onboard oscillator heating up. At 14:08:34 UTC ERT, we reduced the number of phased antennas from 19 antennas to 12 antennas (removing some of the outer arm antennas). Although this reduces the total gain of the system, it increases the size of the phased beam (allowing for positional uncertainties) and reduces the effects of decoherence due to ionospheric turbulence at low frequencies. A C/No increase of +1.4 dB was observed when the arm antennas were dropped.

Schiaparelli was then observed uninterrupted by GMRT until 14:33:05 UTC when it slewed off-source to recalibrate the array. A C/No increase of +0.5 dB was observed compared to the C/No directly before phasing. The signal was detectable up until 21 s after atmospheric entry (14:52:09 UTC ERT), where it was momentarily lost due to high dynamics and plasma blackout. The signal was reacquired 92 s later and observed until final loss of signal 299 s after entry at 14:57:08 UTC ERT.

This measured EDL Doppler versus predicted is shown in Figure A8. There is an initial large offset in the observed Doppler versus predicted, which is due to the onboard oscillator heating up and stabilizing in frequency. The observed velocity in this plot has been adjusted by −3 parts per million (899 m/s) as per correspondence with Daniel Firre at ESA, as this is the expected frequency offset of the clock at nominal temperature. The last 32 s of detected signal shows an anomalous acceleration, where the line-of-sight velocity of Schiaparelli changed by +42 m/s, yielding an acceleration of approximately +1.3 m/s/s.

The C/No of the carrier as detected at GMRT can be seen in Tables A6 and A7. Generally the C/No was detectable using a spectrogram with 1 s integration times. After GMRT switched to the inner 12 antennas, the C/No was usually around 2–2.5 dB-Hz, and after the Surface Platform LGA was exposed, the C/No increased to 5.0 dB-Hz. An example spectrogram (frequency vs time) can be seen in Figure A9. No Doppler model was applied, x axis is offset from 401.585625 MHz, and all times are in UTC ERT. The green dotted line indicates stationary signal with respect to the surface of Mars, assuming Schiaparelli clock is on-frequency. This spectrogram has been enhanced by removing background noise and overlaying a blue and red trace where the carrier was detected.

6. Conclusion

The JPL and GMRT teams successfully detected the ExoMars Schiaparelli UHF communications signal directly on Earth during TGO/EDM separation on 16 October 2016 and then again during EDL on 19 October 2016. The carrier was observed with a C/No ranging from 1 to 5 dB-Hz. The Doppler shift was observed in real time, allowing operators to detect key events, like atmospheric entry, parachute deploy, and parachute jettison.

The last transmissions received from the lander occurred 14:57:08 UTC ERT, about 22 s before the expected landing time. Just after parachute jettison, during the last 32 s of UHF reception, an anomalous line-of-sight acceleration of +1.3 m/s/s was measured, possibly corresponding to free-fall in Martian gravity as viewed at GMRT.

ESA has since conducted an investigation (Tolker-Nielsen, 2017) and found the root cause of the premature Schiaparelli loss of signal was due to an IMU saturating, causing the vehicle to enter "Terminal Descent" mode early, where the back-shield separated and reaction control system fired rockets for a minimum of 3 s. Once the rockets turned off, Schiaparelli fell to the surface for approximately 34 s.

The real-time relay of the Schiaparelli UHF signal to ESA mission control was invaluable during EDL, providing a crucial first look at the anomaly experienced by the lander. This observation provided the only insight into the event, until hours later, when orbiters like TGO and Mars Express could downlink their EDL-recorded data.

Appendix A: Link Budget Calculation

The system temperature is derived from the nominal temperature of the receiver electronics after adding the galactic background contribution using the known position of Mars with respect to the galactic plane on the day of the landing. We use the 408 MHz all-sky maps of Haslam et al. (1982).

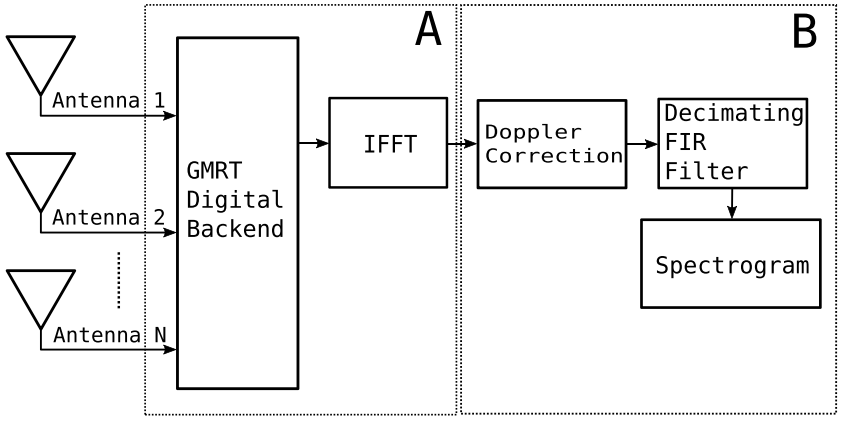

Figure A1. GMRT signal flow for observation of Entry, Descent, and Landing signal. The blocks contained in box A is explained in section 3.1, while box B is explained is section 3.2. GMRT = Giant Metrewave Radio Telescope; IFFT = inverse FFT.

Table A1
Predicted C/No as Received at Giant Metrewave Radio Telescope Using Inner-Arm 12 Antennas During Entry, Descent, and Landing

EDM antenna	Off-boresight (deg)	C/No (dB-Hz)
Backshell LGA	0	7.7
Backshell LGA	45	−0.3 to 5.7
Surface Platform LGA	0	11.9

Note. EDM = Entry, Descent, and LandingDemonstrator Module; LGA = low gain antenna.

Table A2
Mars Science Lab Carrier C/No as Observed at Giant Metrewave Radio Telescope During Multiple Observations in August and October 2016

Date	C/No (dB-Hz)	Antennas
2016-08-23	15.0	22
2016-08-25	16.5	22
2016-08-31	10.0	20
2016-10-05	11.2	13

Note. Dates are in the format of year-month-day.

Table A3
Schiaparelli Separation From TGO Timeline on 16 October 2016

UTC (SCET)	UTC (ERT)	Description
14:26:02	14:35:38	UHF Transmitter On
14:42:00	14:51:36	Separation from TGO
14:57:04	15:06:40	UHF Transmitter Off

Note. TGO = Trace Gas Orbiter; SCET = Spacecraft Event Time; ERT = Earth Receive Time.

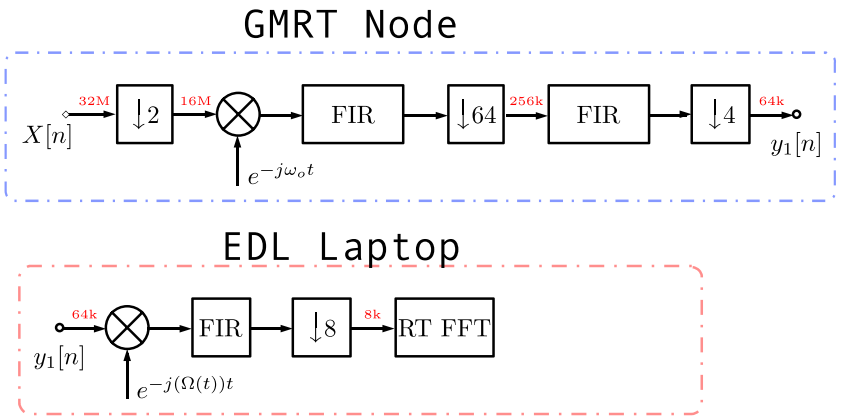

Figure A2. Time domain signal processing. GMRT beam-formed signal is reduced from 32 MHz bandwidth to 8 kHz bandwidth, with resolution bandwidth of 1 Hz centered around the expected carrier frequency. GMRT = Giant Metrewave Radio Telescope; EDL = Entry, Descent, and Landing.

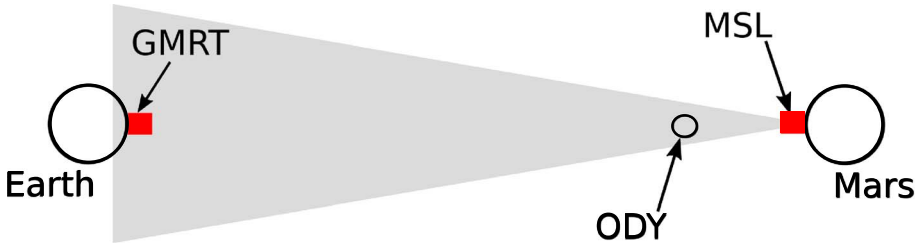

Figure A3. Mars Geometry during tests with MSL, not to scale. Gray cone depicts UHF transmission from Curiosity rover (MSL) to Mars Odyssey (ODY). If Mars is visible in the sky at GMRT then UHF transmissions from MSL can be detected. GMRT = Giant Metrewave Radio Telescope.

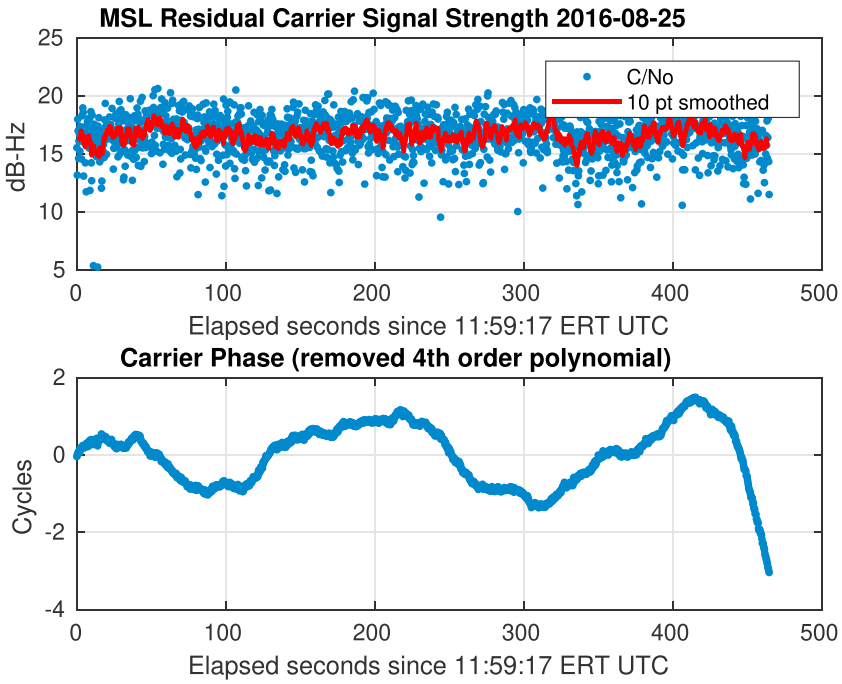

Figure A4. Tracking MSL carrier at Giant Metrewave Radio Telescope on 25 August 2016. Integration time is 0.28 s. ERT = Earth Receive Time.

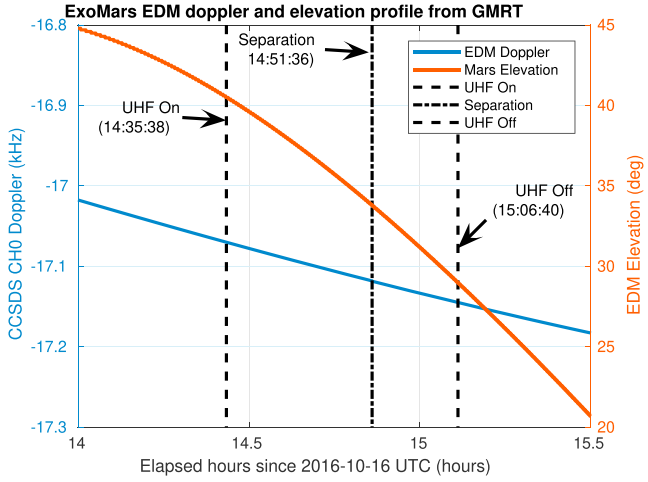

Figure A5. Predicted Schiaparelli separation Doppler and elevation angle as viewed at GMRT, 16 October 2016. All times in UTC Earth Receive Time. EDM = Entry, Descent, and Landing Demonstrator Module; GMRT = Giant Metrewave Radio Telescope.

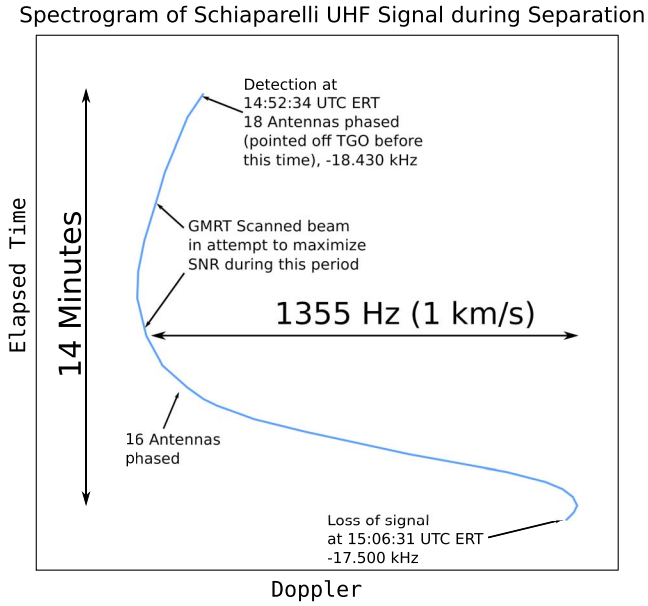

Figure A6. Measured Schiaparelli separation spectrogram on 16 October 2016. ERT = Earth Receive Time; GMRT = Giant Metrewave Radio Telescope.

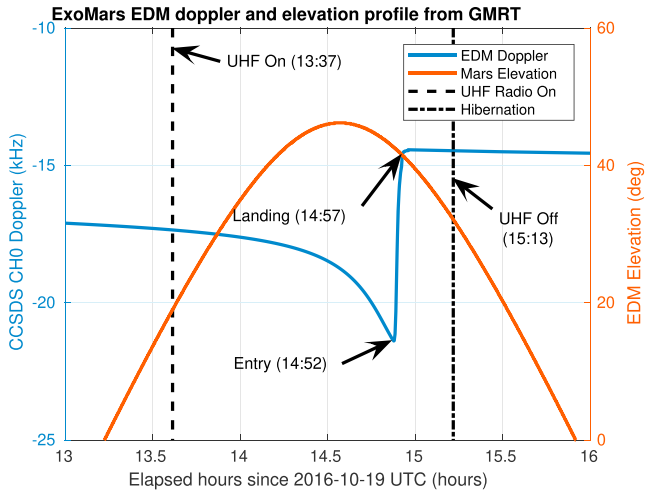

Figure A7. Predicted Schiaparelli Entry, Descent, and Landing Doppler and Elevation angle as observed at GMRT, 19 October 2016. EDM = Entry, Descent, and Landing Demonstrator Module; GMRT = Giant Metrewave Radio Telescope.

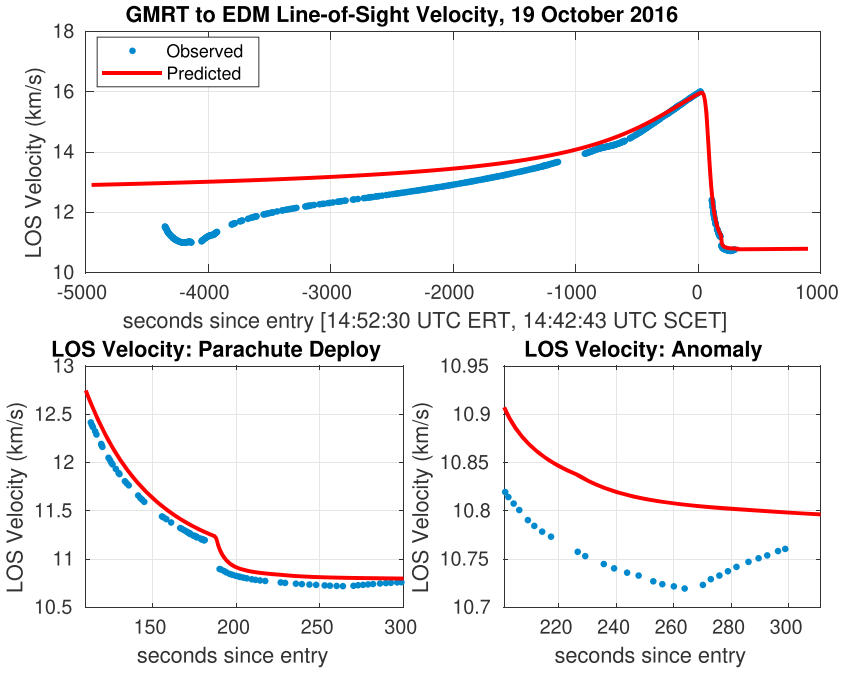

Figure A8. Observed versus predicted Schiaparelli line-of-sight velocity during EDL at GMRT, 19 October 2016. Used European Space Agency-provided predicts GM10-EDM1-2016-293-000000-FD. The observed Doppler shift as been adjusted by −3 ppm (899 m/s) per correspondence with European Space Agency. EDM = Entry, Descent, and Landing Demonstrator Module; GMRT = Giant Metrewave Radio Telescope; ERT = Earth Receive Time; SCET = Spacecraft Event Time.

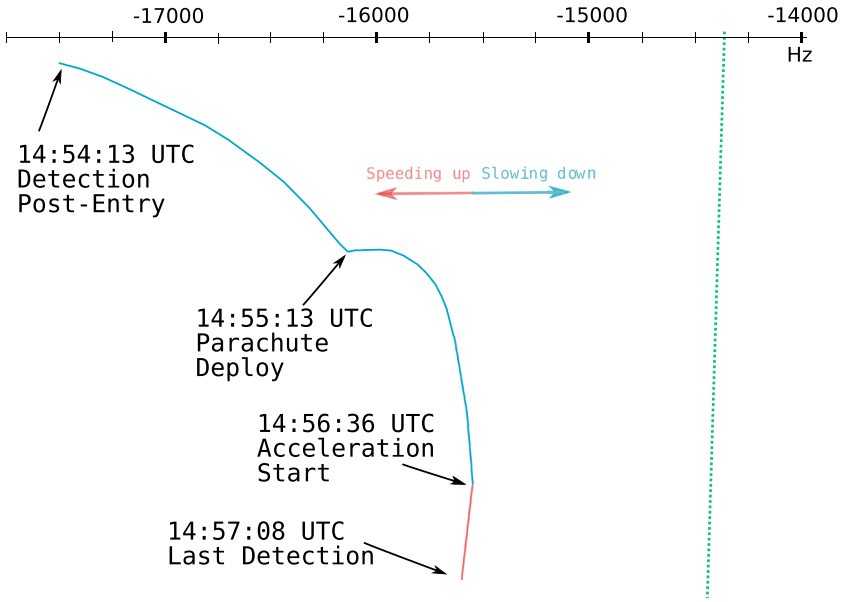

Figure A9. Entry, Descent, and Landing Spectrogram post atmospheric entry as observed at Giant Metrewave Radio Telescope.

Table A4
Schiaparelli Predicted Nominal Entry, Descent, and Landing Timeline on 19 October 2016

UTC (SCET)	UTC (ERT)	Description
13:27:00	13:36:47	UHF Transmitter On
14:42:00	14:51:47	Entry Interface Point (EIP)
14:45:29	14:55:16	Parachute deploy
14:48:05	15:57:52	Touchdown
15:02:00	15:11:47	UHF Transmitter Off

Note. SCET = Spacecraft Event Time; ERT = Earth Receive Time.

Table A5
Schiaparelli Measured EDL Time Line on 19 October 2016 as Observed by GMRT

UTC (SCET)	UTC (ERT)	Description
13:30:44	13:40:31	EDL Carrier Detected
13:58:47	14:08:34	GMRT dropped arm antennas (19 to 12 antennas)
14:23:18	14:33:05	Phasing of GMRT array, 4 min duration
14:42:22	14:52:09	EDM enters Mars atmosphere. (Entry + 0s)
14:42:43	14:52:30	Loss of signal (Entry + 21s)
14:44:15	14:54:02	GMRT reacquires EDM carrier (Entry + 112s)
14:45:23	14:55:10	EDM parachute deploy and loss of signal (Entry + 181s)
14:45:32	14:55:19	GMRT reacquires EDM carrier (Entry + 190s)
14:46:49	14:56:36	EDM parachute jettison, anomalous acceleration starts (Entry + 267s)
14:47:21	14:57:08	Last detection of EDM carrier (Entry + 299s)

Note. EDL = Entry, Descent, and Landing; GMRT = Giant Metrewave Radio Telescope; SCET = Spacecraft Event Time; ERT = Earth Receive Time; EDM = EDL Demonstrator Module.

Table A6
Schiaparelli Carrier C/No as Observed at Giant Metrewave Radio Telescope, 19 October 2016

Time (UTC ERT)	C/No (dB-Hz)	Description
14:00–14:08	1.1	19 Antennas, weak C/No during initial detection
14:11–14:18	2.5	Switch to 12 Antennas
14:33	2.0	Before antenna phasing
14:37	2.5	After antenna phasing
14:55:19	5.0	EDM jettison parachute and backshell

Note. ERT = Earth Receive Time; EDM = Entry, Descent, and Landing Demonstrator Module.

Table A7
Schiaparelli Link Budget Assuming 2 dBiC Low Gain Antenna UHF antenna and Phasing of 12 Inner-Arm Antennas at Giant Metrewave Radio Telescope

Description	dB	Value
TRANSMITTER		
Frequency, MHz		401.59
RF Power, dBm	36.81	
TX Circuit Loss, dB	−3.60	
Antenna Gain, dBi	2.00	
Total EIRP, dBm	35.21	
PATH		
Space Loss, dB	−249.33	
Range, AU		1.16
Atmospheric Atten, dB	−0.62	
Total, dBm	−249.95	
RECEIVER		
Number of antennas		12.00
Polarization Loss, dB	−0.50	
Antenna Gain, dBi	53.32	
Antenna diameter, m		45.00
Efficiency		0.50
Pointing Loss, dB	−0.50	
Noise Density, dBm/Hz	−176.15	
Galactic Noise, K		55.00
System Temp, K		121.00
POWER (Pt)		
Received Power, dBm	−162.41	
Received Pt/N0, dB-Hz	13.73	
RESIDUAL CARRIER (Pr)		
TLM mod index, deg		60.00
Carrier suppression	−6.02	
Received Pr/N0, dB-Hz	7.71	

Acknowledgments
The authors would like to thank Daniel Firre at ESA for providing data on Schiaparelli. Chad Edwards, Dong Shin, Ben Bradley, Roy Gladden, Shan Malhotra at JPL for helping the team with coordination with ESA, MSL + orbiter predictions, and MAROS/MPX interface. Retzler Andrs for providing the amazing csdr (https://github.com/simonyiszk/csdr) open source package used for signal processing. We thank Swarna K. Ghosh and the staff of GMRT who made these observations possible. The GMRT is run by the National Center for Radio Astrophysics of the Tata Institute of Fundamental Research. The research described in this paper was carried out at the Jet Propulsion Laboratory, California Institute of Technology, under a contract with the National Aeronautics and Space Administration.

References

Asmar, S., Esterhuizen, S., Gupta, Y., De, K., Firre, D., Edwards, C., & Ferri, F. (2017). Direct-to-Earth radio link from the ExoMars Schiaparelli Lander. In *14th International Planetary Probe Workshop*. The Hague, Netherlands.

Bell, D., Allen, S., Chamberlain, N., Danos, M., Edwards, C., Gladden, R., & Thomas, R. (2014). MRO relay telecom support of Mars Science Laboratory surface operations. In *2014 IEEE Aerospace Conference*, (pp. 1–10). Big Sky, MT. https://doi.org/10.1109/ AERO.2014.6836170

De, K., & Gupta, Y. (2016). A real-time coherent dedispersion pipeline for the giant metrewave radio telescope. *Experimental Astronomy*, *41*, 67–93. https:doi.org/10.1007/s10686-015-9476-8

Folkner, W. M., Asmar, S. W., Border, J. S., Franklin, G. W., Finley, S. G., Gorelik, J., & Tyler, G. L. (2006). Winds on Titan from ground-based tracking of the Huygens probe. *Journal of Geophysical Research*, *111*, E07S02. https:doi.org/10.1029/2005JE002649

Gupta, Y., Kramer, M., & Wex, N. (2000). IAU Colloquium 177: Pulsar Astronomy: 2000 and beyond. *Publications of the Astronomical Society of the Pacific*, *112*(768), 280. http://stacks.iop.org/1538-3873/112/i=768/a=280

Haslam, C. G. T., Salter, C. J., Stoffel, H., & Wilson, W. E. (1982). A 408 MHz all-sky continuum survey. II - The atlas of contour maps. *Astronomy and Astrophysics Supplementary Series* , *47*, 1–142.

Kornfeld, R. P., Bruvold, K. N., Morabito, D. D., Craig, L. E., Asmar, S. W., & Ilott, P. A. (2011). Reconstruction of Entry, Descent and Landing communications for the Phoenix Mars Lander. *Journal of Spacecraft and Rockets*, *48*, 822–835. https:doi.org/10.2514/1.47909

Makovsky, A., Ilott, P., & Taylor, J. (2009). Mars science laboratory telecommunications system design. Descanso Design and Performance Summary Series.

Oudrhiri, K., Asmar, S., Estabrook, P., Kahan, D., Mukai, R., Ilott, P., & Shidner, J. (2013). Sleuthing the MSL EDL performance from an X band carrier perspective. In *2013 IEEE Aerospace Conference*, (pp. 1–13). Big Sky, MT. https:doi.org/10.1109/AERO.2013.6497418

Roy, J., Gupta, Y., Pen, U. L., Peterson, J. B., Kudale, S., & Kodilkar, J. (2010). A real-time software backend for the GMRT. *Experimental Astronomy*, *28*, 25–60. https:doi.org/10.1007/s10686-010-9187-0

Schratz, B. C., Soriano, M., Ilott, P., Shidner, J., Chen, A., & Bruvold, K. (2014). Telecommunications performance during Entry, Descent, and Landing of the Mars Science Laboratory. *Journal of Spacecraft and Rockets*, *51*(4), 1237–1250. https:doi.org/10.2514/1.a32790

Soriano, M., Finley, S., Fort, D., Schratz, B., Ilott, P., Mukai, R., & Satorius, E. (2013). Direct-to-Earth communications with Mars Science Laboratory during Entry, Descent, and Landing. In *2013 IEEE Aerospace Conference*. Big Sky, MT. https:doi.org/10.1109/AERO.2013.6496816

Swarup, G. (1997). Feasibility study for Low-Cost Parabolic Dishes, 12–25 m diameter. In *The URSI Large Telescope Working Group Meeting and 1kT International Technical Workshop*. Sydney, Australia.

Tolker-Nielsen, T. (2017). EXOMARS 2016 - Schiaparelli Anomaly Inquiry. ESA, DG-I/2017/546/TTN.

Witasse, O., Lebreton, J., Bird, M. K., Dutta-Roy, R., Folkner, W. M., Preston, R. A., & Laux, C. (2006). Overview of the coordinated ground-based observations of Titan during the Huygens mission. *Journal of Geophysical Research*, *111*, E07S01. https:doi.org/10.1029/2005JE002640